ESI to accompany:

Red emitting $[Ir(C^N)_2(N^N)]^+$ complexes employing bidentate 2,2':6,2''-terpyridine ligands for light-emitting electrochemical cells

Edwin. C. Constable,[a] Catherine E. Housecroft,[a]* Gabriel E. Schneider,[a] Jennifer A. Zampese,[a] Henk J. Bolink,*[b,c] Antonio Pertegás[b] and Cristina Roldan-Carmona[b]

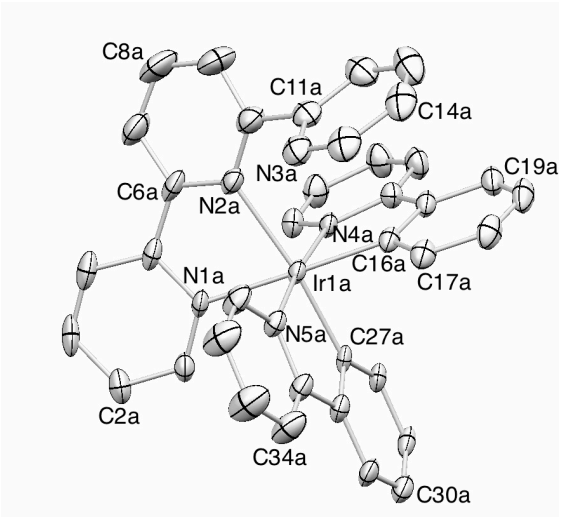

Fig. S1. Structure of one of two independent $[Ir(ppy)_2(tpy)]^+$ cations in $4\{[Ir(ppy)_2(tpy)][PF_6]\}\cdot 2.5Et_2O\cdot 1.5MeCN\cdot 3H_2O$. Ellipsoids plotted at 30% probability level; H atoms omitted. Selected bond lengths: Ir1a–N1a = 2.130(5), Ir1a–N2a = 2.214(5), Ir1a–C27a = 1.994(6), Ir1a–C16a = 2.018(6), Ir1a–N5a = 2.042(5), Ir1a–N4a = 2.049(5) Å.

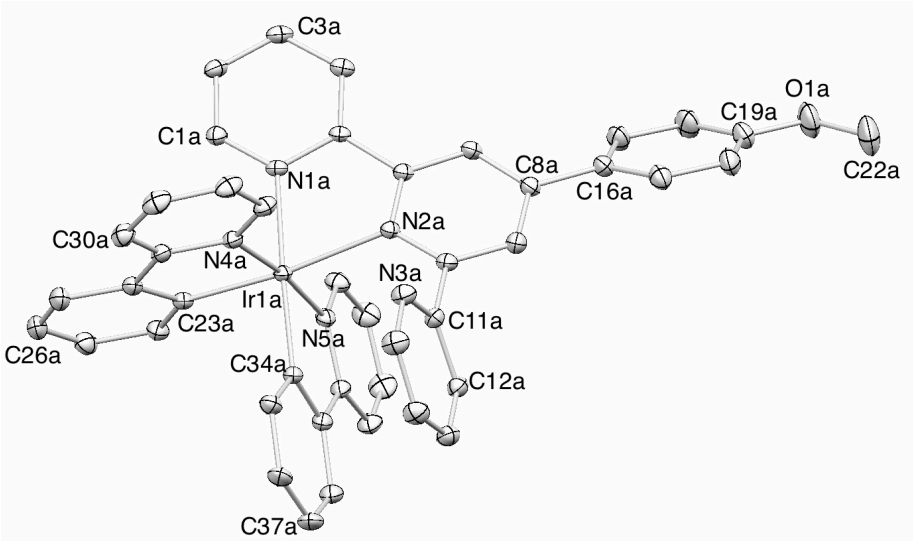

Fig. S2. Structure of one of two independent $[Ir(ppy)_2(\mathbf{2})]^+$ cations in $4\{[Ir(ppy)_2(\mathbf{2})][PF_6]\}\cdot Et_2O\cdot 2MeCN$. Ellipsoids plotted at 30% probability level; H atoms omitted. Selected bond lengths: Ir1a–C23a = 1.996(3), Ir1a–C34a = 2.015(3), Ir1a–N4a = 2.039(2), Ir1a–N5A = 2.058(2), Ir1a–N1a = 2.122(2), Ir1a–N2a = 2.206(2) Å.

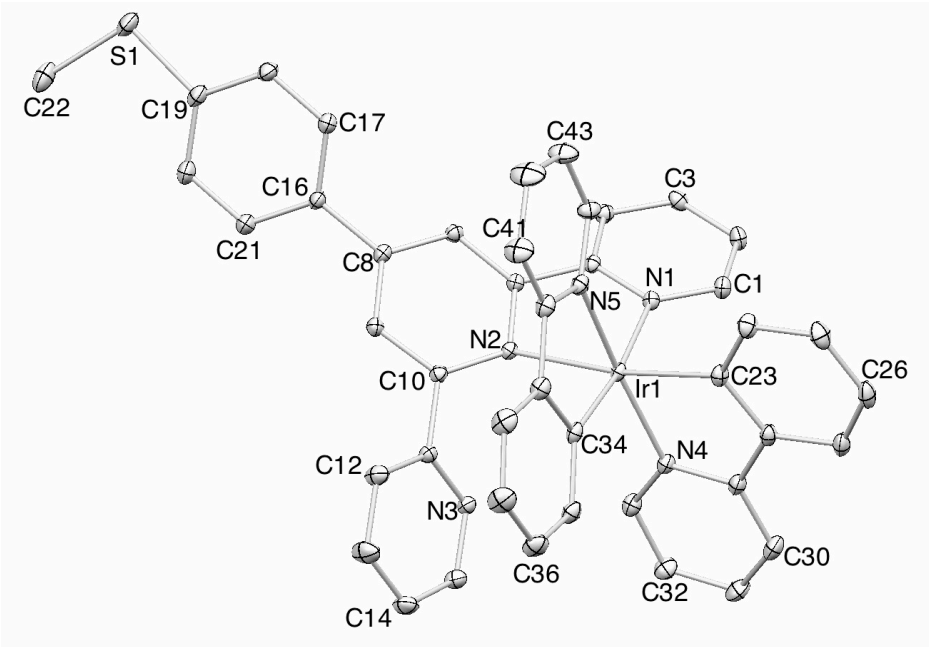

Fig. S3. Structure of the $[Ir(ppy)_2(\mathbf{3})]^+$ cation in $2\{[Ir(ppy)_2(\mathbf{3})][PF_6]\}\cdot MeCN\cdot H_2O$ with ellipsoids plotted at 30% probability level; H atoms omitted. Selected bond lengths: Ir1–C23 = 2.0037(12), Ir1–C34 = 2.0140(14), Ir1–N5 = 2.0504(12), Ir1–N4 = 2.0533(11), Ir1–N1 = 2.1291(11), Ir1–N2 = 2.2300(10) Å.

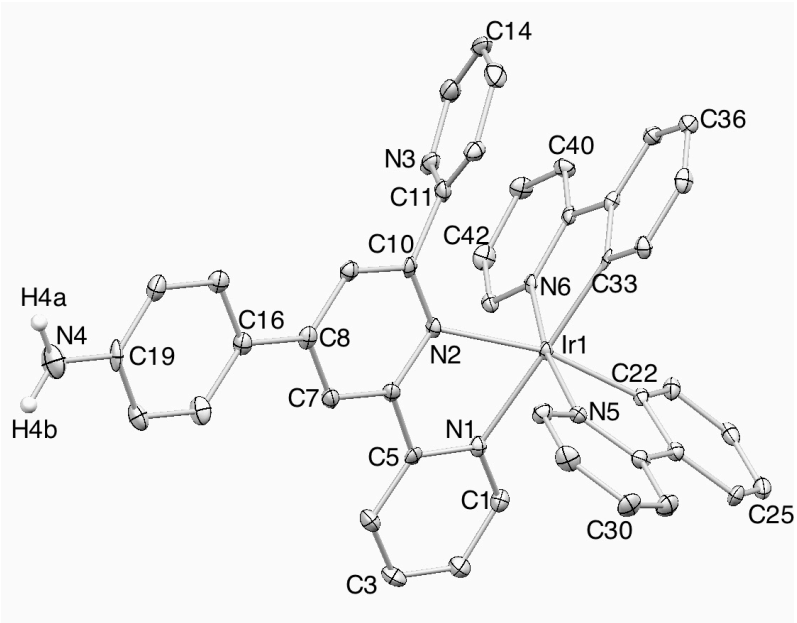

Fig. S4. Structure of the $[Ir(ppy)_2(\mathbf{4})]^+$ cation in $[Ir(ppy)_2(\mathbf{4})][PF_6]\cdot 2CH_2Cl_2$ with ellipsoids plotted at 30% probability level; H atoms except those in the NH_2 unit are omitted. Selected bond lengths: Ir1–C33 = 2.012(5), Ir1–C22 = 2.013(5), Ir1–N6 = 2.039(4), Ir1–N5 = 2.057(4), Ir1–N1 = 2.153(4), Ir1–N2 = 2.204(4) Å.

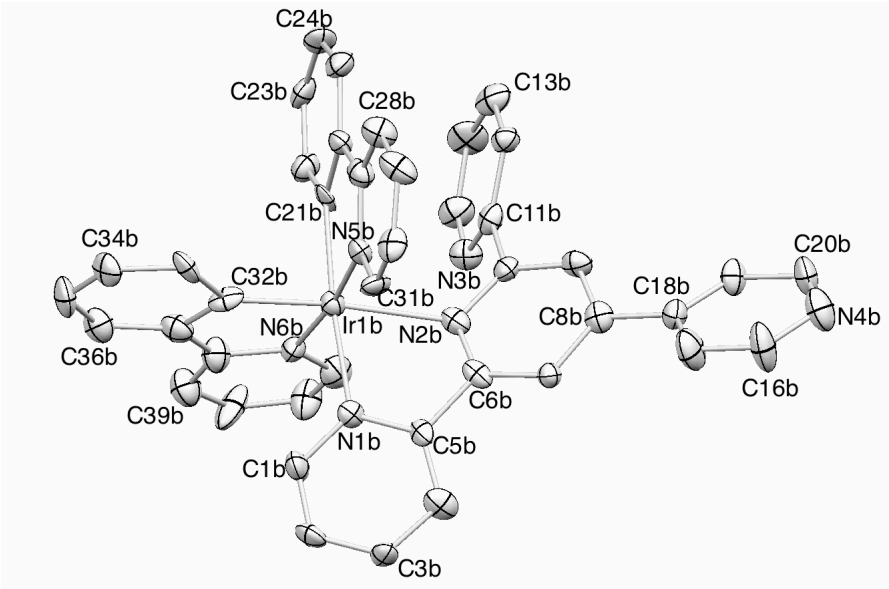

Fig. S5. Structure of one of two independent $[Ir(ppy)_2(pytpy)]^+$ cations in $2\{[Ir(ppy)_2(pytpy)][PF_6]\}\cdot Et_2O\cdot CH_2Cl_2$. Ellipsoids plotted at 30% probability level and H atoms omitted. Selected bond lengths: Ir1b–C32b = 1.929(17), Ir1b–C21b = 1.978(15), Ir1b–N5b = 2.034(13), Ir1b–N6b = 2.043(13), Ir1b–N1b = 2.115(12), Ir1b–N2b = 2.214(14) Å.

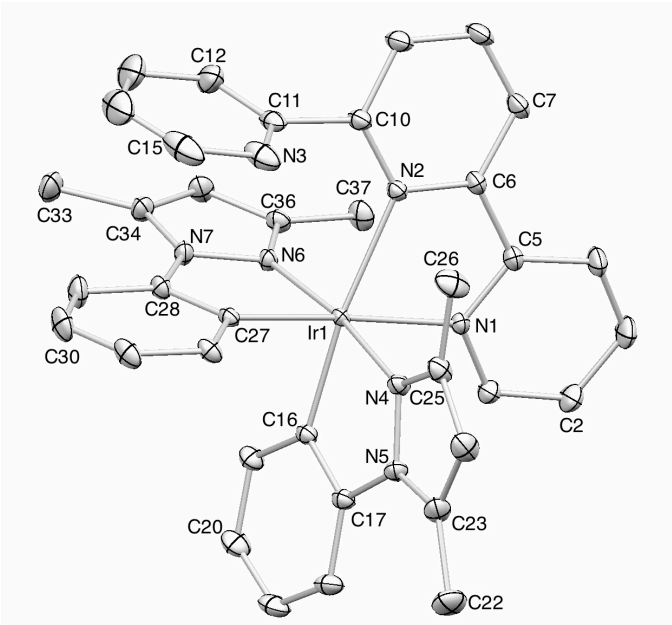

Fig. S6. Structure of the $[Ir(dmppz)_2(tpy)]^+$ cation in $[Ir(dmppz)_2(tpy)][PF_6]$ with ellipsoids plotted at 30% probability level and H atoms omitted. Selected bond lengths: Ir1–C16 = 2.0030(19), Ir1–C27 = 2.011(2), Ir1–N6 = 2.0250(17), Ir1–N4 = 2.0281(18), Ir1–N1 = 2.1402(17), Ir1–N2 = 2.2212(17) Å.

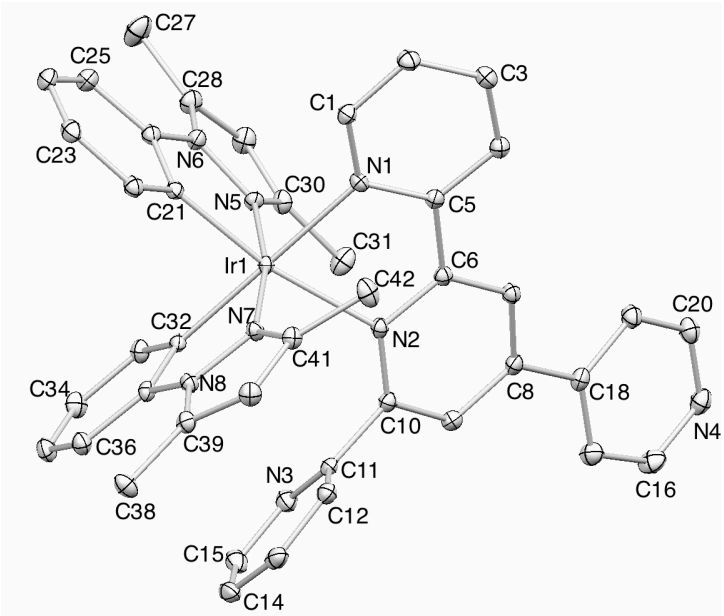

Fig. S7. Structure of the $[Ir(dmppz)_2(pytpy)]^+$ cation in $[Ir(dmppz)_2(pytpy)][PF_6]\cdot CH_2Cl_2$; ellipsoids plotted at 30% probability level and H atoms omitted. Selected bond lengths: Ir1–C21 = 2.008(3), Ir1–C32 = 2.015(2), Ir1–N7 = 2.031(2), Ir1–N5 = 2.051(2), Ir1–N1 = 2.134(2), Ir1–N2 = 2.206(2) Å.

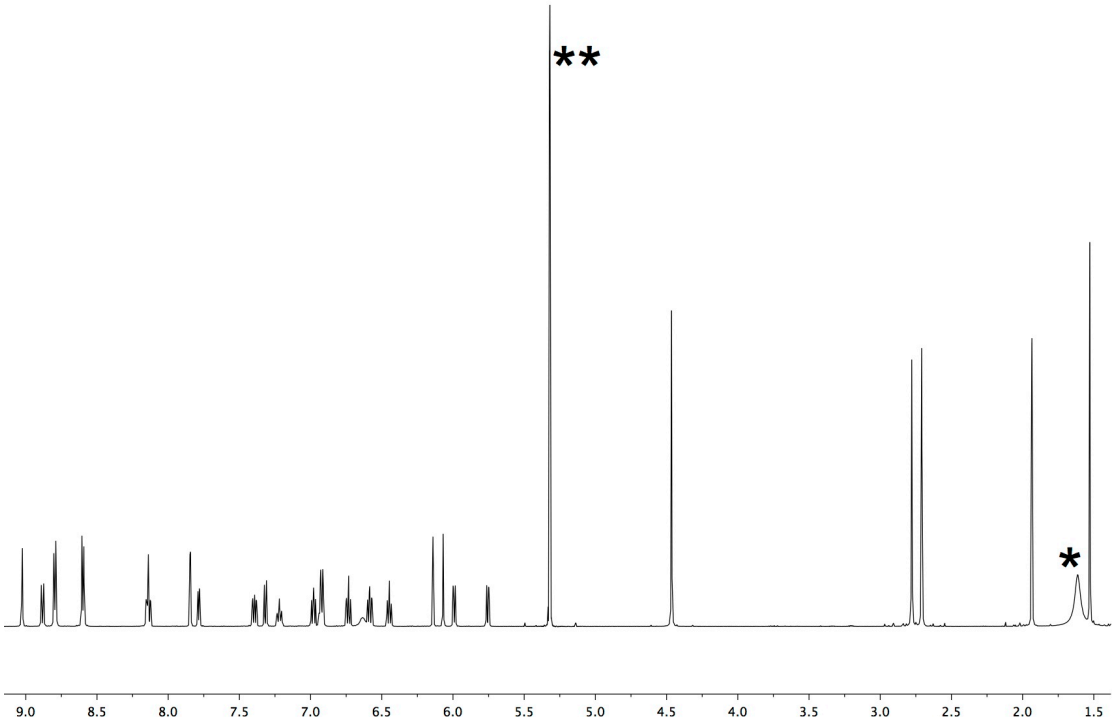

Fig. S8 500 MHz ^1H NMR spectrum of $[Ir(dmppz)_2(Mepytpy)][PF_6]_2$ ($CDCl_3$, 295 K). Peaks marked ** and * are residual $CHCl_3$ and H_2O respectively.

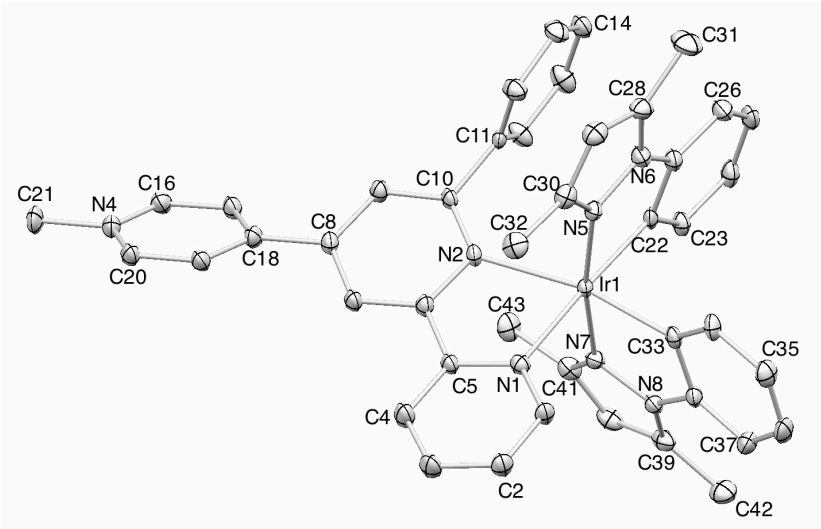

Fig. S9. Structure of the $[Ir(dmppz)_2(Mepytpy)]^{2+}$ cation in $[Ir(dmppz)_2(Mepytpy)][PF_6]_2{\cdot}2CH_2Cl_2$; ellipsoids plotted at 30% probability level and H atoms omitted. Selected bond lengths: Ir1–C33 1.991(5), Ir1–N5 = 2.018(5), Ir1–C22 = 2.024(5), Ir1–N7 = 2.044(4), Ir1–N1 = 2.152(4), Ir1–N2 = 2.214(4) Å.

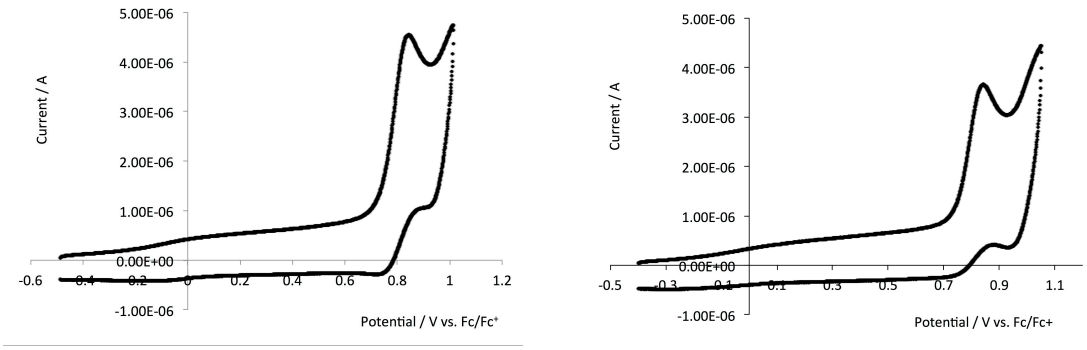

(a) (b)

Fig. S10 Sweep to positive potential in the cyclic voltammograms of (a) $[Ir(ppy)_2(\mathbf{2})][PF_6]$ and (b) $[Ir(dmppz)_2(tpy)][PF_6]$ (with respect to Fc/Fc^+; CH_2Cl_2 solution) showing the quasi-reversible process.

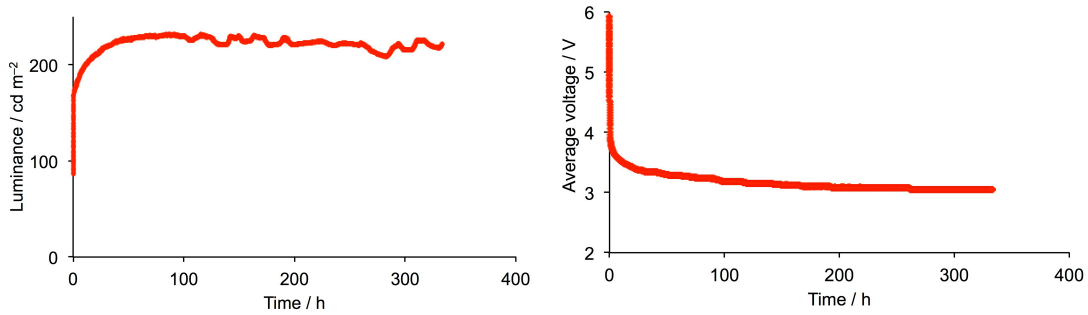

(a) (b)

Fig S11. The device performance of the $[Ir(ppy)_2(6\text{-Phbpy})][PF_6]$ under the pulsed driving conditions, analogous to those used for the best preforming devices in this paper. (a) Luminance, and (b) average voltage versus time.

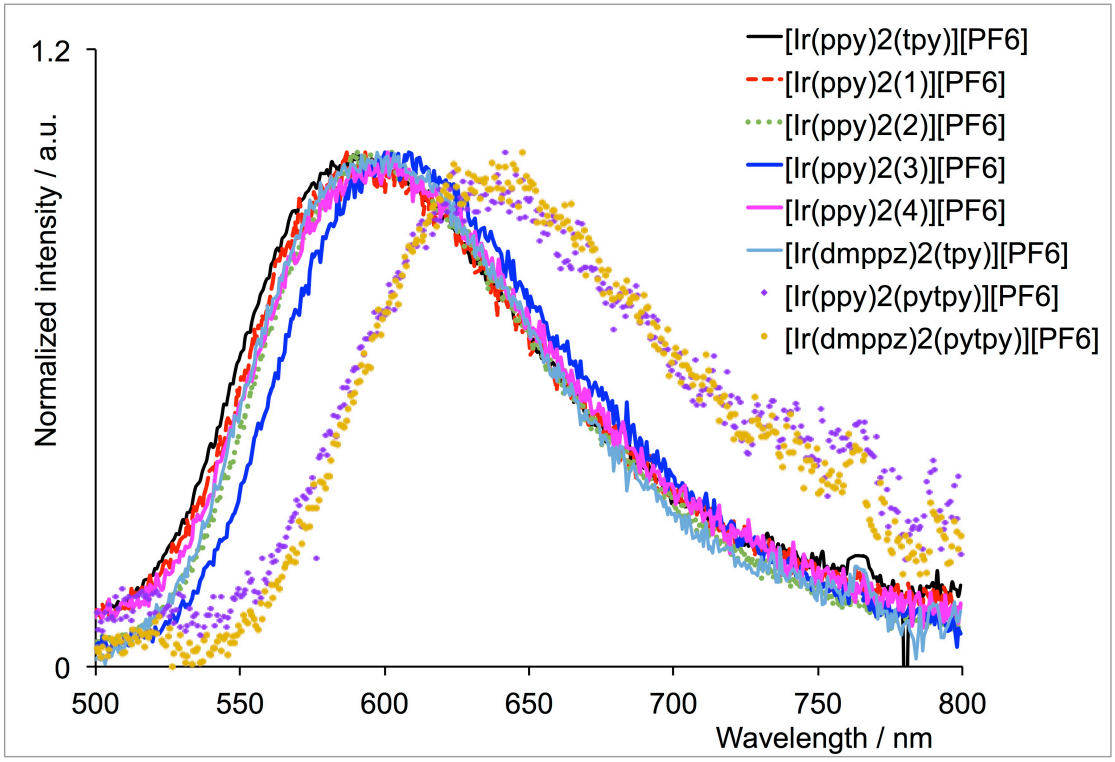

Fig. S12. Photoluminescence spectra in thin films (iTMC:IL 4:1).